IOP Publishing Semiconductor Science and Technology
Semicond. Sci. Technol. **36** (2021) 065012 (10pp) https://doi.org/10.1088/1361-6641/abf46d

Improvement in Schottky barrier inhomogeneities of Ni/AlGaN/GaN Schottky diodes after cumulative γ-ray irradiation

Ajay Kumar Visvkarma[1,2], Chandan Sharma[3], Chanchal Saraswat[2], D S Rawal[2,*], Seema Vinayak[2] and Manoj Saxena[4]

[1] Semiconductor Device Research Laboratory, Department of Electronic Science, University of Delhi, South Campus, New Delhi 110021, India
[2] MMIC Fabrication Division, Solid State Physics Laboratory, New Delhi 110054, India
[3] Department of Physics, Indian Institute of Technology, New Delhi 110016, India
[4] Deen Dayal Upadhyaya College, University of Delhi, New Delhi 110078, India

E-mail: dsrawal15@gmail.com

Received 11 December 2020, revised 29 March 2021
Accepted for publication 1 April 2021
Published 7 May 2021

Abstract

This article reports the effect of gamma (γ)-ray irradiation on barrier inhomogeneities that leads towards improvement in diode parameters in Ni-AlGaN/GaN Schottky diodes. The Schottky diodes were subjected to a cumulative γ-ray dose up to 15 kGy and their current–voltage (I–V) and capacitance–voltage (C–V) characteristics were measured simultaneously at different temperatures during the pristine stage and after each radiation dose. The Schottky barrier height (Φ_b) had an increase of 10% to 20% in the temperature range greater than 250 K. Whereas, the change in the ideality factor (η) was found to be prevalent at lower temperatures (<250 K). More linearity in the behavior of η variation with temperature was found post γ-irradiation showing an improvement in homogeneity of the metal/semiconductor interface. Post γ-ray exposure, barrier inhomogeneities at the metal/semiconductor interface were found to reduce due to annealing effects that also led towards an increase in the contribution of thermionic emission current flow. Further, a decrease of 16% in the standard deviation of the Gaussian distribution of Φ_b around the mean Φ_b was obtained. A decrease in contact resistance (R_C) was deduced using a circular transmission line method, which was also due to the partial annealing effect of γ-ray radiation. Finally, the channel carrier concentration (n_s), extracted using C–V analysis, was found to remain unaltered.

Keywords: AlGaN/GaN diodes, gamma irradiation, I–V–T characterization, barrier inhomogeneity, ηkT vs kT curve

(Some figures may appear in colour only in the online journal)

1. Introduction

Gallium nitride (GaN) has been recognized as an eminent material with its superior material properties in comparison to conventional semiconductors. GaN falls into the category of wide band-gap semiconductors with an electronic band-gap of 3.4 eV [1]. Due to the strong bonding between gallium and nitrogen atoms [2] it can sustain higher temperatures and is also considered to be a very radiation hard material in comparison to the other conventionally used semiconductors like Si, Ge and GaAs. Due to its radiation hardness properties,

* Author to whom any correspondence should be addressed.

GaN material becomes more noticeable in space applications. Devices based on GaN material, such as high electron mobility transistors (HEMTs), have already established their significance in various domains, such as in high-frequency/high-power applications, solid-state lightening, sensors and nuclear reactors [3–9]. Just because any material is radiation hard (GaN here), it does not imply that the devices fabricated on that material can sustain the equivalent amount of radiation. Post radiation several physical changes exist that lead to device failure, such as deterioration of contact pads, material degradation and degradation in metal/semiconductor (M/S) interfaces [10, 11]. For possible space application, the effects of different radiations that include electrons, protons, neutrons and γ-rays on GaN-based devices are of major interest. A consolidated amount of literature is available on proton, electron and neutron radiation effects on GaN-based devices [12–15]. Whereas, in the case of γ-radiation a wide spectrum of literature exists stating the harnessing as well as degradation of GaN material and/or GaN-based devices [16–20]. In our earlier studies, the impacts of γ-ray irradiation on GaN material properties and on different AlGaN/GaN-based devices are reported. Further, a link is also established between changes found in GaN material properties to the changes observed in electrical characteristics of different GaN-based devices such as HEMTs and Schottky diodes [11, 21–23]. In particular, for GaN Schottky diodes, Membreno *et al* reported an increase in Φ_b after γ-radiation (dose 210 kGy) treatment but did not account for the presence of barrier inhomogeneities [24]. Similarly, in their study of quasi-vertical Schottky GaN diodes Bian *et al* showed an improvement in Φ_b and η post γ-ray exposure up to 10 kGy dose. They also included only a qualitative insight into the presence of barrier inhomogeneities [25]. Our previous publication includes only the dimension-dependent effect of gamma radiation on Schottky contact parameters and ohmic contact parameters. Post γ-irradiation improvement in η is also reported without taking into account the effect of barrier inhomogeneities [22]. To the best of our knowledge, a quantitative analysis on the effect of γ-ray irradiation on barrier inhomogeneities in a Schottky M/S interface is still not reported.

This article reports the impact of γ-ray irradiation on M/S interface properties, more precisely nickel Schottky diodes on an AlGaN/GaN epitaxial hetero-structure, using current–voltage measurements by varying temperature (I–V–T) analysis. An AlGaN/GaN hetero-structure is being studied instead of metal/GaN or metal/AlGaN structures because the application of this analysis can be directly linked to the Schottky gate of AlGaN/GaN HEMTs and also, in the M/S case, the semiconductors are taken as bulk crystals with doping that may deviate from current results and may not give its direct relation to GaN hetero-structure-based HEMT devices. The temperature dependence of Φ_b and η is extracted. The spread of the non-linear dependence of η with temperature indicates that the M/S interface is inhomogeneous and is therefore non-ideal behavior of the Schottky diode. After γ-ray irradiation the spread in η values is found to reduce, therefore showing an improvement in the M/S interface properties in terms of a reduction in barrier inhomogeneities.

2. Experimental procedure

The different area Schottky diodes including Ni/Au metal were fabricated over an $Al_{0.24}Ga_{0.76}N$/GaN epitaxial HEMT structure grown using a standard metal organic chemical vapor deposition technique [26]. The epitaxial layers include a 27 nm $Al_{0.24}Ga_{0.76}N$ barrier layer over a 2 μm GaN buffer layer separated by a 1 nm AlN spacer layer in between the barrier and buffer layer. The electron concentration (n_s) and mobility (μ) were determined using contactless Hall measurement and were found to be $\sim 8.5 \times 10^{12}$ cm^2 and 1850 cm^2 V^{-1} s^{-1}.

The fabrication of Schottky diodes started with the definition and deposition of an ohmic metal stack using an optical lithography procedure and electron beam (e-beam) evaporation, respectively. A Ti/Al/Ni/Au metal stack of thickness 320 nm was deposited and then annealed at 820 °C for 90 s (in nitrogen ambient) in a rapid thermal annealing system. Post mesa isolation, a metal scheme including Ni/Au of thickness 40 nm/200 nm was deposited using the same e-beam evaporation system for Schottky contacts. Next, for γ-ray radiation the sample was transferred to a 'Gamma chamber (GC) 5000' equipped with ^{60}Co source with photon energies of 1.17 MeV and 1.33 MeV. The source had a dose rate of 0.467 kGy h^{-1} during the irradiation process. The sample was irradiated cumulatively with successive doses of 1 kGy, 4 kGy and 10 kGy at room temperature under normal atmospheric conditions. Electrical measurements that include circular transmission line method (C-TLM) measurement and a Schottky diode I–V at different temperatures (I–V–T) were recorded at the pristine stage and after each γ-ray irradiation dose. A schematic of the experiment is shown in figure 1(a), whereas the actual fabricated different area Schottky diodes are shown in figure 1(b).

3. Results and discussion

To understand the effects of γ-radiation on the M/S interface, careful I–V–T measurements were performed during the pristine stage as well as after each radiation dose. The sample was placed in a closed chamber under vacuum of 9.33×10^{-6} mbar, equipped with a liquid nitrogen cooled cryostat with a temperature range from 77 K to 350 K. I–V–T characteristics of the Schottky diode (area 100×100 μm^2) were recorded using Keithley's semiconductor device analyzer (4200-SCS) during the pristine stage and are shown in figure 2, and the corresponding extracted parameters that include Φ_b, η and diode series resistance (R_D) are shown in table 1.

The thermionic emission (TE) model is used to calculate the Φ_b, η and R_D using standard diode equations (1) and (2):

$$I = I_S \left[\exp\left(\frac{qV - IR_D}{\eta kT} \right) - 1 \right] \tag{1}$$

$$I_S = AA^*T^2 \exp\left(-q\Phi_b/kT\right) \tag{2}$$

where I_s is the reverse saturation current, Φ_b is the barrier height, A is the area of the diode (1.0×10^{-4} cm^2), A^* is the Richardson constant for the AlGaN barrier layer, η is the

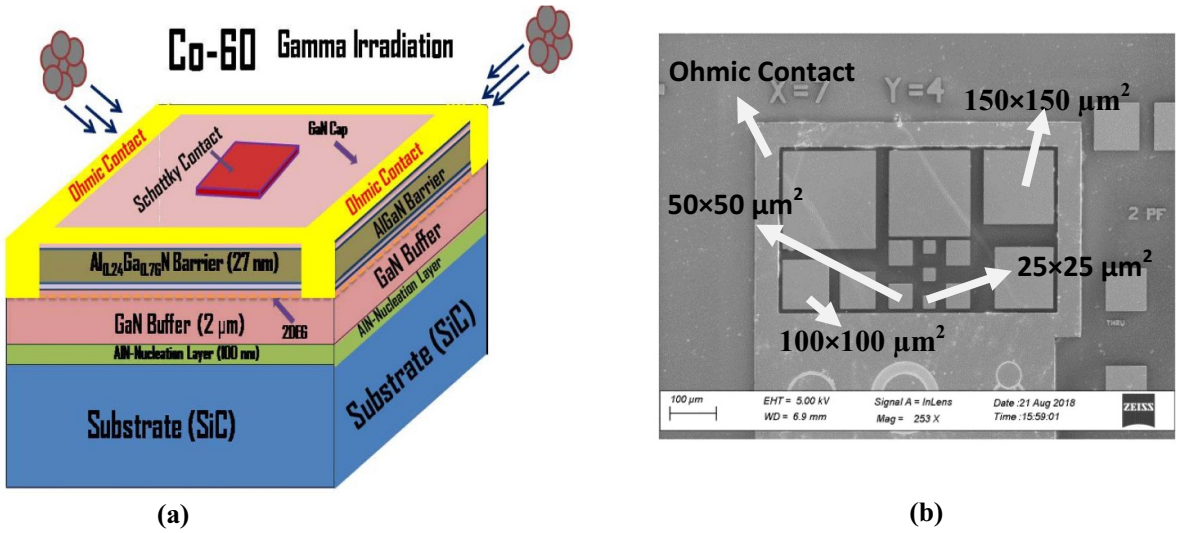

Figure 1. (a). A simplified schematic of the Ni/AlGaN/GaN Schottky diode under γ-exposure. (b) An SEM micrograph of fabricated different area Schottky diodes.

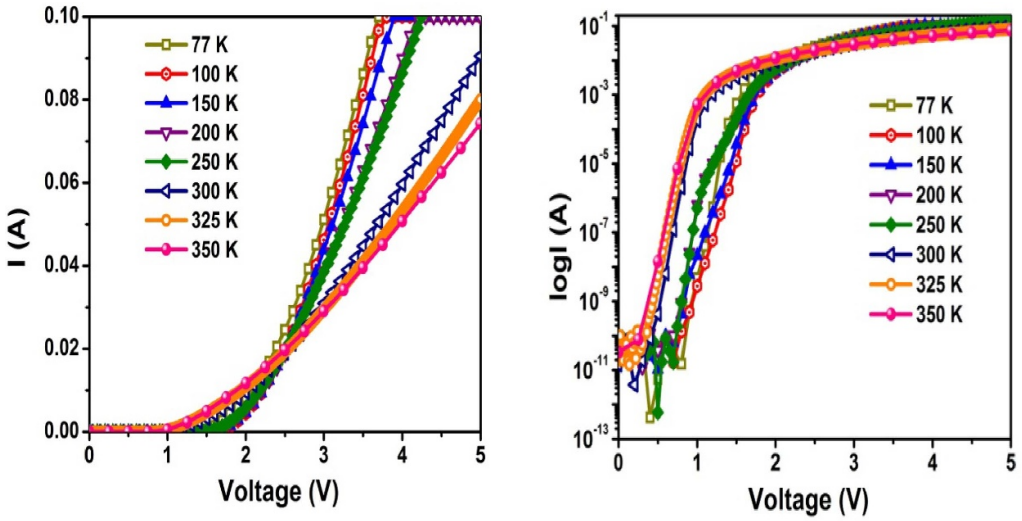

Figure 2. *I–V–T* forward characteristics of the 100 × 100 μm^2 area Schottky diode in linear and log scale.

Table 1. The extracted Φ_b, η and R_D during the pristine stage using *I–V–T* characteristics.

Temperature (K)	Φ_b (eV)	η	R_D (Ω)
77	0.32	7.67	9.5
100	0.34	7.16	10.7
150	0.49	4.80	11.5
200	0.78	2.20	13.9
250	0.85	2.05	17.3
300	0.92	1.54	22.9
325	1.05	1.39	28.3
350	1.05	1.48	34.4

ideality factor, q is elementary charge, k is Boltzmann's constant and T is the temperature of the measurement [27]. Here, IR_D is the voltage drop across the diode, and R_D is determined between the voltage range of 2.5 V to 4 V. Similarly, Φ_b and η are calculated between the voltage range of 0.5 V to 1.5 V with an error count of $\pm$0.02 for Φ_b and $\pm$0.03 for η, respectively.

The calculated values of Φ_b, η and R_D had shown a remarkable change after the 2nd dose (5 kGy) and 3rd dose (15 kGy) of γ-ray irradiation and are shown in figures 3(a) and (b) and in table 2. The change in Φ_b is in between 10% and 20% in the temperature ranges greater than 250 K. Further, a spread in extracted values of Φ_b and η with variation in temperature can be seen during the pristine stage, which was then reduced after successive γ-ray exposures (see figure 3(a) and table 2).

According to the TE model, in an ideal Schottky contact Φ_b and η should not vary with temperature. The variation of Φ_b and η with temperature indicates the presence of non-idealities at the Schottky interface/junction [28–34]. Schottky barrier formation at the M/S interface includes different non-idealities, such as (a) impurity atoms or dangling bonds

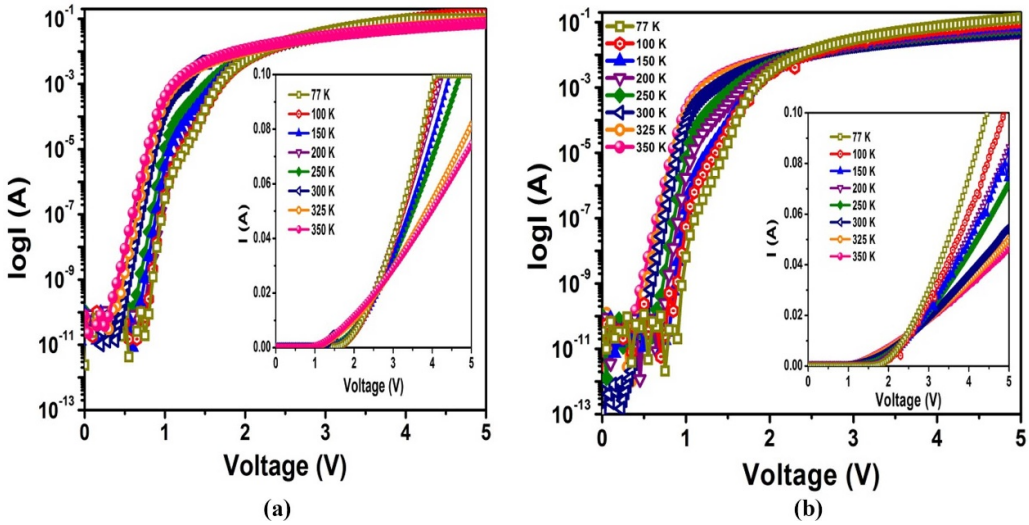

Figure 3. (a). *I–V–T* forward characteristics after 1 kGy + 4 kGy = 5 kGy dose in the 100 × 100 μm^2 area Schottky diode. (b) *I–V–T* forward characteristics after 1 kGy + 4 kGy + 10 kGy = 15 kGy dose in the 100 × 100 μm^2 area Schottky diode.

Table 2. Comparisons of the calculated Φ_b, η and R_D after cumulative γ-ray irradiation.

	η			Φ_b (eV)			R_D (Ω)		
Temperature (K)	1 kGy	5 kGy	15 kGy	1 kGy	5 kGy	15 kGy	1 kGy	5 kGy	15 kGy
77 K	7.42	4.35	4.20	0.36	0.35	0.38	9.0	9.1	11.0
100 K	6.80	3.90	3.41	0.38	0.42	0.47	9.4	10.1	13.4
150 K	4.51	2.55	2.35	0.52	0.62	0.69	11.5	12.6	16.8
200 K	2.25	1.93	1.81	0.80	0.85	0.89	14.9	16.5	19.0
250 K	2.03	1.70	1.56	0.84	0.95	1.01	20.7	23.1	27.1
300 K	1.52	1.43	1.39	0.92	1.06	1.12	26.8	30.3	39.2
325 K	1.41	1.28	1.29	1.06	1.09	1.13	30.6	35.3	45.2
350 K	1.50	1.36	1.30	1.07	1.12	1.14	36.0	39.1	49.0

of atoms at the semiconductor surface or loosely bonded M/S atoms, (b) a tunneling current in addition to a thermionic current, (c) generation–recombination current in the depletion region and (d) image force lowering of the barrier at the M/S interface [27, 35]. These non-idealities lead towards inhomogeneous metal contact, and therefore find the scope to become more homogeneous with physical or chemical treatments, such as annealing of contacts after metal deposition or pre-metal treatments with plasma or wet chemicals [36–38].

As shown in figure 4(a), the change found in η was greater in the low temperature range (<250 K) during the pristine stage as well as after different radiation doses. This change in η (or spread in η) was reduced after exposure to γ-radiation that qualitatively points towards a decrease in barrier inhomogeneities. This reduction in η is due to the annealing effects of γ-radiation, as described in our previous work [11, 22, 23]. Further, figure 4(b) corroborates the qualitative confirmation of improvement in non-idealities at the M/S junction. After gamma radiation exposure the spread in Φ_b remains almost the same with a shift towards the higher values side (10%–20% higher than pristine values).

Again, at lower temperatures there are two slopes visible in *I–V* curves for the pristine stage as well as after γ-radiation exposure. The expected reasons for this observation are related either to the series resistance or due to a change in the current transport mechanism at lower temperatures. Since, after γ-ray exposure, there is an improvement in η values indicating that the contribution of the TE current has increased over other current transport mechanisms a change in slope can therefore be expected.

As per the TE model, Φ_b and η are independent of temperature and, therefore, ηkT vs kT should have a linear dependence. The deviation from linearity implies the presence of more than one current transport mechanism due to the presence of non-idealities at the M/S junction [27, 30]. Figure 4(b) shows that after the 3rd dose of γ-ray irradiation (15 kGy), the ηkT vs kT curve becomes more linear, and therefore confirms the reduction in non-idealities with suppression of other current transport mechanisms. This is due to annealing effects of γ-ray radiation leading towards an improvement in surface and interface properties of the Ni/AlGaN contact and AlGaN/GaN heterointerface [21–23]. In the temperature range greater than 250 K the change in η was smaller, therefore suggesting that the non-idealities were less active in this range [28–30].

Similar observations in parameter η were also recorded in Schottky diodes of different areas (see figure 5). As in the case of η, similar behavior of the spread in extracted values of Φ_b was found during the pristine stage and after different radiation

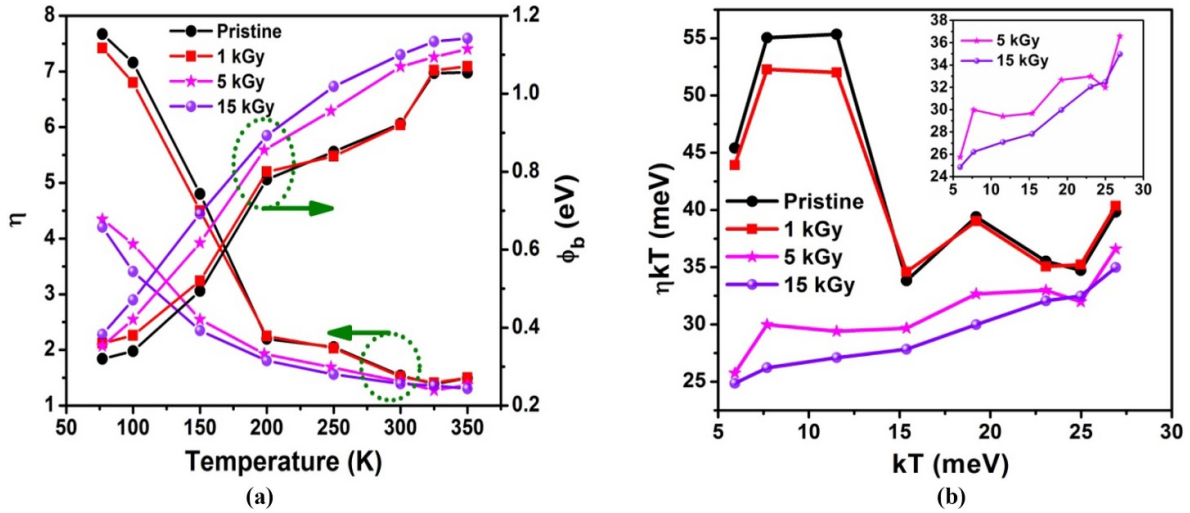

Figure 4. (a). Comparison of Φ_b and the ideality factor after each cumulative γ-ray dose. (b) A comparison of ηkT vs kT plot after γ-irradiation.

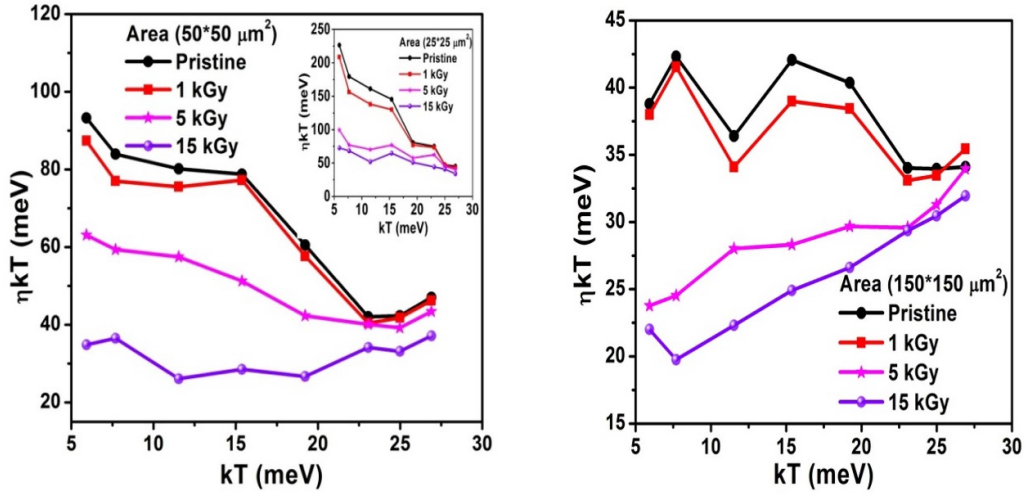

Figure 5. Comparisons of ηkT vs kT plots after γ-irradiation of different area Schottky diodes.

doses with a shift towards higher values with temperature variation (figure 3(a)). Considering the non-idealities due to an inhomogeneous interface at the M/S junction, the effective single Schottky barrier which is reflected in the *I–V* characteristics is a summary of a number of independent Schottky barriers with variable barrier heights. The junction current flows through all such diodes of different barrier heights and, as per the TE theory, the ratio of the junction current through the high to low Schottky barrier region is $\exp(-q(\phi_{b,high} - \phi_{b,low})/kT)$. This junction current gets altered with a radiation dose leading to an effective shift in Φ_b towards higher values [32].

Since Φ_b and η were found to vary with temperature the M/S interface was therefore not homogeneous. Next, a Gaussian distribution of Schottky barrier height across the M/S junction was considered [39], which is based on the analytical potential fluctuation model given by Werner and Guttler [35]. The Gaussian distribution $p(\phi_b)$ of Schottky barriers at the Ni/AlGaN M/S interface [33, 35] is given by equation (3) below:

$$p(\phi_b) = \frac{1}{\sigma_0\sqrt{2\pi}}\exp\left[-\frac{(\phi_b - \bar{\phi_{B0}})^2}{2\sigma_0^2}\right] \tag{3}$$

where $\bar{\phi_{B0}}$ is the mean Schottky barrier height, and σ_0 is the standard deviation around the mean Schottky barrier height ($\bar{\phi_{B0}}$).The total current density across the junction with inhomogeneities is expressed as

$$I(V) = \int_{-\infty}^{\infty} I(\phi_b, V)\, p(\phi_b)\, d\phi_b \tag{4}$$

where $I(\phi_b, V)$ is the current at voltage bias V for a Φ_b based on the TE theory. From equations (1)–(4), we obtain $I(V)$ with a modified barrier given as

$$I(V) = I_s \exp\left(\frac{qV}{\eta_{ap}kT}\right)\left[1 - \exp\left(-\frac{qV}{kT}\right)\right] \tag{5}$$

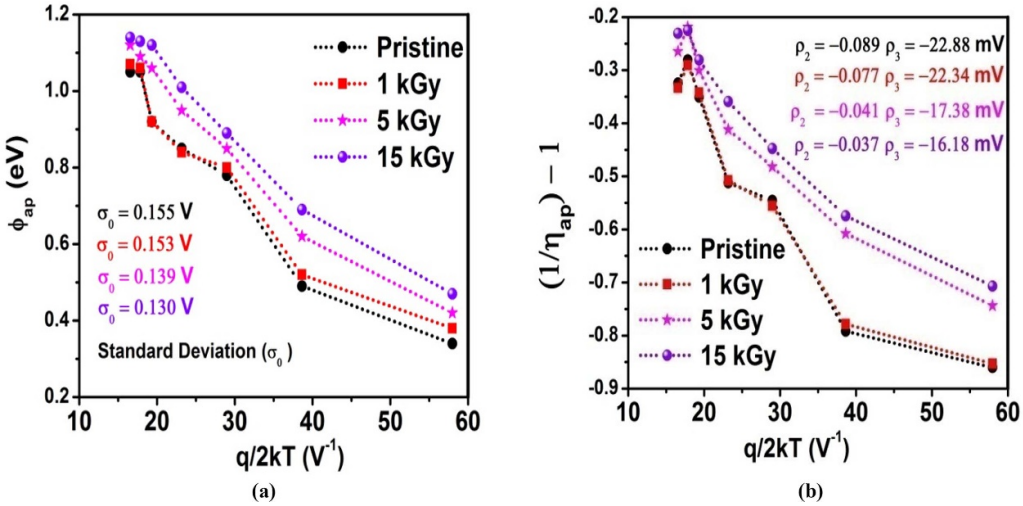

Figure 6. Extraction of Gaussian distribution parameters: (a) standard deviation around the mean value of Φ_b, (b) bias dependent coefficients around the mean Φ_b and the standard deviation.

$$I_S = AA^*T^2\exp\left(-\frac{q\Phi_{ap}}{kT}\right) \tag{6}$$

where Φ_{ap} and η_{ap} are the apparent Schottky barrier height and ideality factor as seen from the measured I–V characteristics and with the incorporation of interface barrier inhomogeneities expressed by equations (7) and (8) [33, 35]:

$$\Phi_{ap}\ (T) = \phi_{B0}^{-} - \frac{q\sigma_0^2}{2kT} \tag{7}$$

$$\left(\frac{1}{\eta_{ap}} - 1\right) = -\rho_2 + \frac{q\rho_3}{2kT} \tag{8}$$

where ρ_2 and ρ_3 are voltage bias coefficients. According to the Werner model, ϕ_{B0}^{-} and σ_0 are the linear function of Gaussian parameters (ρ_2 and ρ_3). Hence, Φ_{ap} and η_{ap} were plotted against $q/2kT$ with cumulative γ-irradiation doses and are shown in figures 6(a) and (b). The curves were fitted between the most linear region (16 V^{-1}–40 V^{-1}) to extract σ_0 and other Gaussian parameters, ρ_2 and ρ_3. A decrease in σ_0 and an increase in Gaussian parameters was found with each successive γ-ray dose. In comparison to the pristine stage an improvement of 16% in σ_0 was observed after the 3rd γ-ray dose. Further, the increase found in the coefficients ρ_2 and $\rho_3$means more ideal behavior in diode characteristics with fewer inhomogeneities. This shows that gamma radiation results in improvement in Schottky barrier inhomogeneities at the M/S interface. Similar behavior showing a decrease in σ_0 was calculated after successive γ-irradiation in other area diodes and is shown in figure 7 and in table 3.

Since the extracted values of σ_0 are quite high along with a wide spread in Φ_{ap} and $\eta_{ap,}$ it is evident that the assumed current transport mechanism is not purely the TE emission current. This leads to possible exploration of other current transport mechanisms in addition to the pure TE mechanism [40, 41]. This kind of behavior in AlGaN/GaN Schottky diodes is also observed by Kim *et al* [42] and Sheoran *et al* [43] on

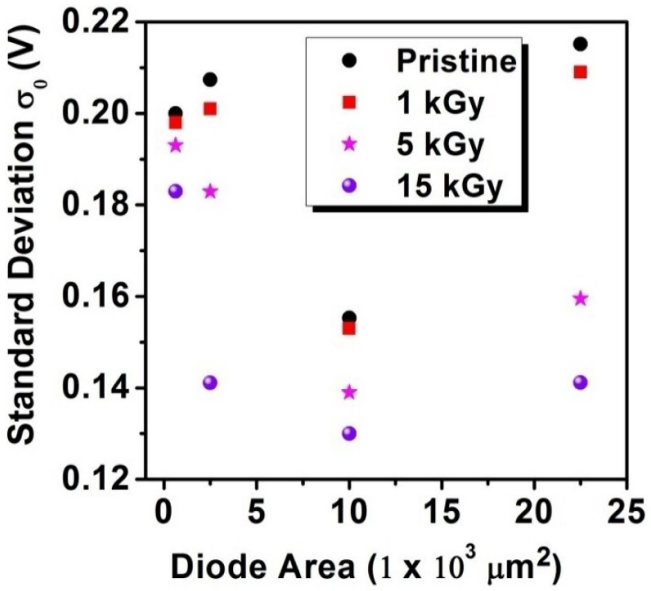

Figure 7. The extracted standard deviation (σ_0) from equation (7) for different area Schottky diodes under consideration.

Table 3. Extracted values for σ_0 from equation (7) for different area Schottky diodes.

	σ_0 (V)				
Area (μm^2)	Pristine	1 kGy	5 kGy	15 kGy	% change in σ_0
25 × 25	0.200	0.198	0.193	0.183	8.5
50 × 50	0.207	0.201	0.183	0.141	31
100 × 100	0.155	0.153	0.139	0.130	16
150 × 150	0.215	0.209	0.159	0.141	34

Ga_2O_3 wide band-gap material with a comparable value of σ_0. Again, the tunneling current equation given by Rideout and Crowell [44] includes the tunneling probability (E_0) as

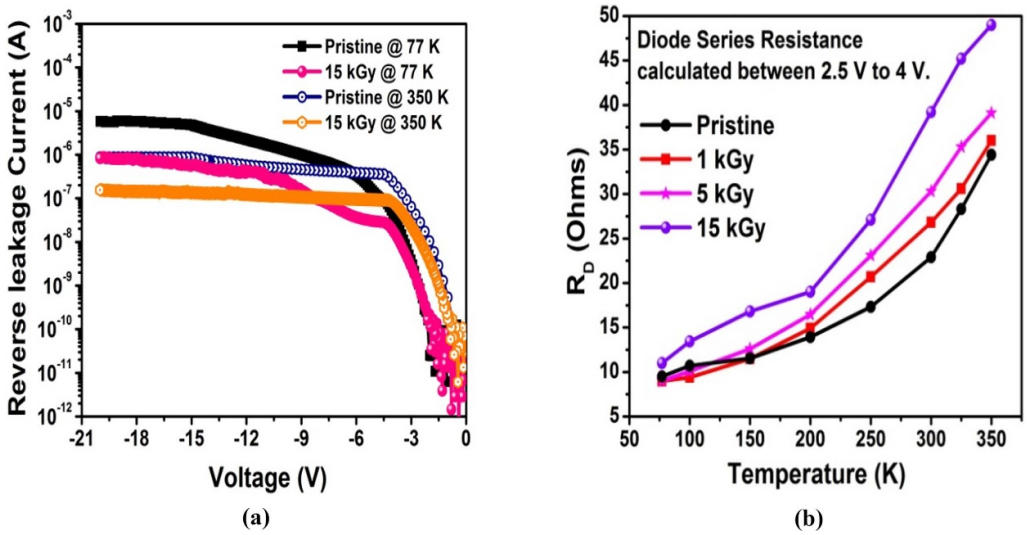

Figure 8. (a). Schottky reverse characteristics after 1 kGy + 4 kGy + 10 kGy = 15 kGy dose at 77 K and 350 K. (b) Diode series resistance after 1 kGy + 4 kGy + 10 kGy = 15 kGy dose.

$E_0 = E_{00}\coth(E_{00}/kT)$, where E_{00} is a material-dependent energy constant given as

$$E_{00} = \frac{qh}{4\pi}\left[\frac{N}{m*\varepsilon_s}\right]^{1/2} \tag{9}$$

where N is the donor concentration, m^* is the effective mass, h is Planck's constant, q is elementary charge and ε_s is semiconductor permittivity. In our case AlGaN/GaN are unintentionally doped semiconductors with a two-dimensional electron gas (2DEG) channel at the interface. This channel concentration remained unaltered during the experiment (confirmed by C–V measurements) and, hence, E_{00} becomes a constant term making the tunneling probability only dependent on temperature. It is known that the tunneling current dominates at low temperature due to an increase in tunneling probability in comparison to thermionic current and, due to this shift, the extracted Schottky parameters through the TE model are the resulting high values of ideality factors at low temperatures.

Next, the diode reverse leakage current (I_{leakage}) is plotted in figure 8(a) for the pristine stage and after the 3rd dose (15 kGy) of irradiation for temperatures of 77 K and 350 K. An improvement in I_{leakage} was recorded after gamma radiation exposure. This was expected due to the combined effect of the increase in Φ_b and the improvement in η values, and the same is also reported in our previous studies [22].

R_D was calculated for a higher voltage range (2.5 V and 4 V) and is shown in figure 8(b). The cause of diode resistance is the depletion region formation at the M/S interface. This depletion region acts as barrier to the flow of electric charges and therefore offers resistance [27]. When charge carriers cross this depletion region they collide with atoms and charge carriers present at the interface resulting in a decrease in their energies. Also, the presence of surface states and impurity atoms at the Schottky junction also act as a conducting path to the charge carries [27]. As we discussed previously, due to γ-ray exposure these colliding sites and surface states at the M/S junction get modified and re-arranged and are therefore reflected as an improvement in barrier inhomogeneities. This contributes towards a change in R_D. In addition to an increase in Φ_b and a decrease in barrier inhomogeneities, the increase found in R_D also contributes to the improvement in the reverse leakage current.

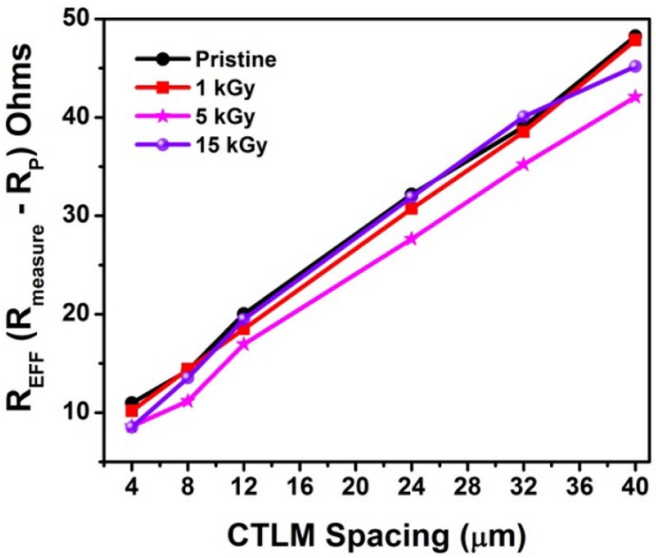

Figure 9. The variation in C-TLM resistance data with cumulative γ-ray irradiation.

The effect of the same γ-ray dose exposure on contact resistance (R_C) and the figure of merit (FOM) was also characterized using the C-TLM method [22] and is shown in figure 9. The changes calculated in values of C-TLM data during the pristine stage and after irradiation are shown in table 4. As mentioned there, R_p is the probe resistance, whereas R_{EFF} is ($R_{measured} - R_p$). R_C and FOM were improved post γ-ray exposure due to the localized partial annealing of the ohmic stack. The localized annealing due to irradiation is similar

Table 4. CTLM measurements before and after γ-ray irradiation.

	Pristine stage				1 kGy		5 kGy		10 kGy	
Spacing (μm)	R_p (Ω)	R_{EFF} (Ω)	R_c (Ω)	FOM (Ω mm)	R_c (Ω)	FOM (Ω mm)	Rc (Ω)	FOM (Ω mm)	R_c (Ω)	FOM (Ω mm)
4	3.08	14.07	1.98	0.62	1.54	0.48	1.23	0.39	1.15	0.36
8	3.08	17.35								
12	3.08	23.10								
24	3.08	35.25								
32	3.08	42.14								
40	3.08	51.35								

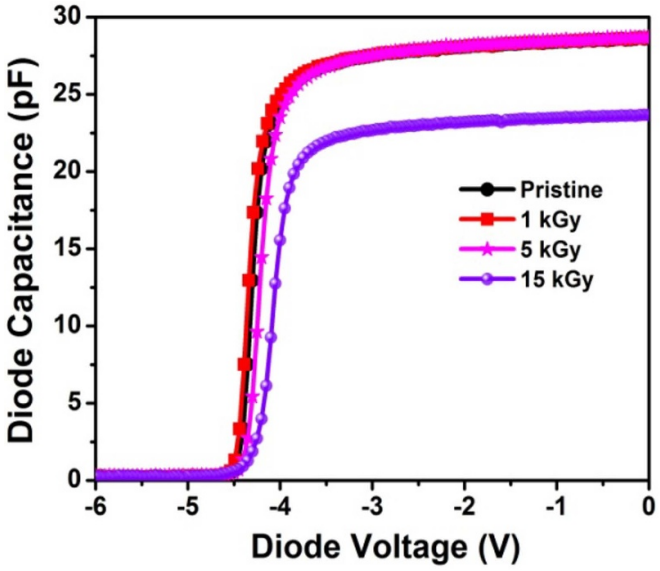

Figure 10. *C–V* characteristics of the Schottky diode (area 100×100 μm^2) under test with cumulative γ-ray irradiation.

to infrared radiation annealing carried out for ohmic contact formation with 2DEG [11, 22, 23].

Towards the end, the 2DEG carrier concentration (n_s) was extracted using *C–V* analysis using equation (10) [22]:

$$n_s = \int N(w)\,\mathrm{d}w = \frac{2}{q\varepsilon A^2 d\,(1/C^2)/\mathrm{d}V} \qquad (10)$$

where *N(w)* is the 2DEG carrier concentration in per cubic cm, *W* is the depletion width, *A* is the Schottky pad area, *q* is the elementary charge and ε is the permittivity of the AlGaN barrier layer.

The *C–V* plots given in figure 10 were measured at room temperature. During an applied reverse bias of -3 V to -5 V the depletion region gradually reaches the AlGaN/GaN interface where the 2DEG channel is present. This reverse field depletes the carriers away from the channel, and therefore a drop in junction capacitance is observed. Moreover, since each Schottky contact is encircled completely by ohmic contact the leakage current is minimized, and therefore a sharp drop in junction capacitance was observed between the reverse bias of -3 V to -5 V.

Table 5. Extracted V_P and n_s parameters from *C–V* analysis.

	Pristine	1 kGy	5 kGy	15 kGy
V_P (V)	-4.43	-4.44	-4.39	-4.27
n_S (cm^{-2})	7.40×10^{12}	7.48×10^{12}	7.30×10^{12}	5.86×10^{12}

The measured capacitance value showed a decrease in the maximum capacitance value ($\sim$20% in the accumulation region) only after 15 kGy of gamma radiation exposure. The calculated n_s values are shown in table 5 along with the pinch off voltage (V_P). No appreciable change in n_s (since the order of n_s is the same) was found post gamma radiation exposure showing that the 2DEG carrier concentration remains unaltered after irradiation. However, a small shift of around 3.5% in V_P was observed post 15 kGy dose. This positive shift in V_P along with a decrease in capacitance is due to rearrangement of already present traps/defects below the Schottky gate region [11, 22, 23]. However, the decrease in capacitance is in the pico-Farad scale and has no major impact on the device characteristics. Moreover, in our previous work it was also found that post successive incremental radiation 3–4 times in same sample leads towards initiation of fluctuation in various measured/calculated parameters (such as capacitance in this case) due to degradation found in contact metal pads [11].

4. Conclusion

The impact of γ-irradiation on Schottky diodes fabricated on an AlGaN/GaN hetero-structure was studied using a cumulative γ-ray dose regime. The diodes' electrical characteristics were recorded under variable temperature ranges post different doses of γ-ray irradiation. Variations in Φ_b, η, R_D and $I_{leakage}$ were found after γ-ray exposure. In the lower temperature range (<250 K) the changes in η were greater in comparison to the higher temperature range, whereas the changes in Φ_b were more pronounced at temperatures greater than 250 K. It is observed that the spread of diode parameters (Φ_b, η and R_D) in the measured temperature range (77 K–350 K) has decreased after successive doses of gamma radiation. These changes found in diode *I–V* parameters were due to improvement in M/S interface properties and a decrease in barrier inhomogeneities, which are evident from ηkT vs kT linear behavior. A Gaussian distribution of Schottky barriers was considered to incorporate the effect of barrier inhomogeneities at the M/S

interface. An improvement of 16% was observed in the standard deviation of the Gaussian distribution around the mean Φ_b after the final γ-ray dose (15 kGy). Next, the C-TLM measurements post radiation infers refinement of R_C. Finally, *C–V* analysis confirms no change in 2DEG carrier concentration after γ-ray exposure confirming that 2DEG remains unaltered post irradiation.

Data availability statement

The data generated and/or analyzed during the current study are not publicly available for legal/ethical reasons but are available from the corresponding author on reasonable request.

Acknowledgments

The authors wish to thank the GaN team, SSPL, Delhi, India for their valuable support and guidance during the execution of this work. The authors are also grateful to the IEEE group, SSPL for IVT measurements and INMAS, Delhi, India for extending the gamma irradiation facility.

ORCID iDs

Ajay Kumar Visvkarma https://orcid.org/0000-0002-2144-3914
Chandan Sharma https://orcid.org/0000-0003-0617-7248
Chanchal Saraswat https://orcid.org/0000-0001-6994-0488
D S Rawal https://orcid.org/0000-0003-4280-2805

References

[1] Pengelly R S, Wood S M, Milligan J W, Sheppard S T and Pribble W L 2012 A review of GaN on SiC high electron-mobility power transistor and MMICs *IEEE Trans. Microwave Theory Tech.* **60** 1764–83
[2] Morkoc H, Cingolani R, Lambrecht W, Gil B, Jiang H-X, Lin J, Pavlidis D and Shenai K 1999 Material properties of GaN in the context of electron devices *Mater. Res. Soc. Internet J. Nitride Semicond. Res.* **4** 18–26
[3] Lovellette M N and Wood K S 2008 High energy gamma rays and modern electronics *IEEE Aerospace Conf.* pp 1–8
[4] Polyakov A Y, Pearton S J, Frenzer P, Ren F, Liu L and Kim J 2013 Radiation effects in GaN materials and devices *J. Mater. Chem.* C **1** 877–87
[5] Su M, Chen C and Rajan S 2013 Prospects for the application of GaN power devices in hybrid electric vehicle drive systems *Semicond. Sci. Technol.* **28** 074012
[6] Nakamura S, Senoh M, Isawa N and Nagahama S 1995 High brightness blue, green and yellow light emitting diodes with quantum well structure *Japan. J. Appl. Phys.* **34** L799
[7] Chung G H, Vuong T A and Kim H 2019 Demonstration of hydrogen sensing operation of AlGaN/GaN HEMT gas sensors in extreme environment *Microarticle* **12** 83–4
[8] Khan M A H and Rao M V 2020 Gallium nitride (GaN) nanostructures and their gas sensing properties: a review *MDPI Sensors* **20** 3889
[9] Sun Y, Kang X, Zheng Y, Lu J, Tian X, Wei K, Wu H, Wang W, Liu X and Zhang G 2019 Review of the recent progress on GaN-based vertical power Schottky barrier diodes (SBDs) *Electronics* **8** 575
[10] Ives N E, Chen J, Witulski A F, Schrimpf R D, Fleetwood D M, Bruce R W, McCurdy M W, Zhang E X and Massengill L W 2015 Effect of proton-induced displacement damage on gallium nitride HEMTs in RF power amplifier applications *IEEE Trans. Nucl. Sci.* **62** 2417–22
[11] Sharma C, Visvkarma A K, Laishram R, Malik A, Narang K, Vinayak S and Singh R 2019 Cumulative dose γ-irradiation effects on material properties of AlGaN/GaN hetero-structures and electrical properties of HEMT devices *Semicond. Sci. Technol.* **34** 065024
[12] Wang C W 2002 Neutron irradiation effect on radio-frequency magnetron-sputtered GaN thin films and Au/GaN Schottky diodes *J. Vac. Sci. Technol.* B **20** 1821
[13] Vitusevich S A, Kurakin A M, Konakova R V, Belyaev A E and Klein N 2008 Improvement of interface properties of AlGaN/GaN heterostructures under gamma-radiation *Appl. Surf. Sci.* **255** 784–6
[14] Pearton S J, Ren F, Patrick E, Law M E and Polyakov A Y 2016 Review-ionizing radiation damage effects on GaN devices *ECS J. Solid State Sci. Technol.* **5** 35–60
[15] Jianxing X, Wang R, Zhang L, Zhang S, Zheng P, Zhang Y, Song Y and Tong X 2020 Early stage degradation related to dislocation evolution in neutron irradiation AlGaN/GaN HEMTs *Appl. Phys. Lett.* **117** 023501
[16] Aktas O, Kuliev A, Kumar V, Schwindt R, Toshkov S, Costescu D, Stubbins J F and Adesida I 2004 60Co gamma radiation effects on DC, RF and pulsed I-V characteristics of AlGaN/GaN HEMTs *Solid-State Electron.* **48** 471–5
[17] Vitusevich S A *et al* 2003 Effects of γ-irradiation on AlGaN/GaN-based HEMTs *Phys. Status Solidi* **195** 101–5
[18] Lee J *et al* 2017 Low dose 60Co gamma-irradiation effects on electronic carrier transport and DC characteristics of AlGaN/GaN high-electron mobility transistors *Radiat. Eff. Defects Solids* **172** 250–6
[19] Hwang Y-H, Hsieh Y L, Lei L, Li S and Ren F 2014 Effects of low dose γ-irradiation on DC performance of circular AlGaN/GaN high electron mobility transistors *J. Vac. Sci. Technol.* B **32** 205–10
[20] Jha S, Jelenkovic E V, Pejovic M M, Ristic G S, Pejovic M, Tong K Y, Surya C, Bello I and Zhang W J 2009 Stability of submicron AlGaN/GaN HEMT devices irradiated by gamma rays *Microelectron. Eng.* **86** 37–40
[21] Sharma C, Modolo N, Wu T-L, Meneghini M, Meneghesso G, Zanoni E, Visvkarma A K, Vinayak S and Singh R 2020 Understanding γ-ray induced instability in AlGaN/GaN HEMTs using a physics-based compact model *IEEE Trans. Electron Devices* **67** 1126–31
[22] Sharma C, Visvkarma A K, Laishram R, Kumar A, Rawal D S, Vinayak S and Singh R 2020 Effects of γ-ray irradiation on Schottky and ohmic contact on AlGaN/GaN hetero-structures *Microelectron. Reliab.* **105** 113565
[23] Sharma C, Singh R, Chao D-S and Tian-Li W 2020 Effects of γ-ray irradiation on AlGaN/GaN heterostructures and high electron mobility transistor devices *J. Electron. Mater.* **49** 6789–97
[24] Umana-Membreno G A, Dell J M, Parish G, Nener B D and Faraone L 2007 Annealing of 60Co gamma radiation-induced damage in n-GaN Schottky barrier diodes *J. Appl. Phys.* **101** 054511
[25] Bian Z *et al* 2020 Gamma irradiation impact on quasi-vertical Schottky barrier diodes *J. Phys. D: Appl. Phys.* **53** 045103
[26] Khan R, Bag R K, Narang K, Pandey A, Dalal S, Singh V K, Saini S K, Padmavati M V G, Tyagi R and Riaz U 2019 Effect of fully strained AlN nucleation layer on the

AlN/SiC interface and subsequent GaN growth on 4H-SiC by MOVPE *J. Mater. Sci., Mater. Electron.* **30** 18910–8
[27] Sze S M 2007 *Physics of Semiconductor Devices* (New York: Wiley)
[28] Gassoumi M 2020 Conductance deep-level transient spectroscopy and current transport mechanisms in Au/Pt/n-GaN Schottky barrier diodes *Phys. Solid State* **62** 636–41
[29] Zeghdar K, Dehimi L, Saadoune A and Sengouga N 2015 Inhomogeneous barrier height effect on the current-voltage characteristics of an Au/n-InP Schottky diode *J. Semiconduct.* **36** 124002
[30] Erdal M O, Kocyigit A and Yildirum M 2019 Temperature dependent current-voltage characteristics of Al/TiO2/n-Si and Al/Cu:TiO2/n-Si devices *Mater. Sci. Semicond. Process.* **103** 104620
[31] Dobrocka E 1994 Influence of barrier height distribution on the parameters of Schottky diodes *Appl. Phys. Lett.* **65** 575–77
[32] Zhou Q *et al* 2019 Barrier inhomogeneity of Schottky diode on non polar AlN grown by physical vapor transport *IEEE J. Electron Devices Soc.* **7** 662–7
[33] Dhimmar J M, Desai H N and Modi B P 2016 Analysis of the inhomogeneous barrier in In/p-Si Schottky contact and modified Richardson plot *J. Nano-Electron. Phys.* **8** 02006
[34] Mostefaoui M *et al* 2014 Current-voltage-temperature (I-V-T) characteristics of Schottky-gate of the structures AlGaN/GaN HEMTs *Sens. Transducers* **27** 280–4
[35] Werner J H and Guttler H H 1991 Barrier inhomogeneities at Schottky contacts *J. Appl. Phys.* **69** 1522–33
[36] Khachariya D, Szymzanski D, Sengupta R, Reddy P, Kohn E, Sitar Z, Collazo R and Palidis S 2020 Chemical treatment effects on Schottky contacts to metal organic chemical vapor deposition n-type N-polar GaN *J. Appl. Phys.* **128** 064501
[37] Diale M and Auret F D 2009 Effects of chemical treatment on barrier height and ideality factor of Au/GaN Schottky diodes *Physica* B **404** 4415–8
[38] Lakshmi Devi V, Jyothi I, Rajagopal Reddy V and Choi C-J 2012 Schottky barrier parameters and interfacial reactions of rapidly annealed Au/Cu bilayer metal scheme on N-type InP *Open Appl. Phys. J.* **5** 1–9
[39] Song Y P, Van Meirhaeghe R L, Laflere W H and Cardon F 1986 On the difference in apparent barrier height as obtained from capacitance-voltage and current–voltage-temperature measurements on Al/p-InP Schottky barriers *Solid State Electron.* **29** 633–8
[40] Yan D, Jiao J, Yang G and Gu X 2013 Forward current transport mechanism in Ni/Au-AlGaN/GaN Schottky diodes *J. Appl. Phys.* **114** 144511
[41] Suzue K, Mohammad S N, FaN Z F, Kim W, Aktas O, Botochkarev A E and Morkoc H 1996 Electrical conduction in platinum-gallium nitride Schottky diodes *J. Appl. Phys.* **80** 4467
[42] Kim H, Choi S and Choi B J 2020 Forward current transport properties of AlGaN/Gan Schottky diodes prepared by atomic layer deposition *Coating* **10** 194
[43] Sheoran H, Tak B R, Manikanthababu N and Singh R 2020 Temperature-dependent electrical characteristics of Ni/Au vertical Schottky barrier diodes on β-Ga_2O_3 epilayers *ECS J. Solid State Sci. Technol.* **9** 055004
[44] Crowell C and Rideout V 1969 Normalized thermionic-field (TF) emission in metal-semiconductor (Schottky) barriers *Solid State Electron.* **12** 89–105